# Resonance Raman examination of axial bonding and spin-state equilibria in metmyoglobin hydroxide and other heme derivatives

2 AUTHORS, INCLUDING:

Sanford A Asher
University of Pittsburgh
**312** PUBLICATIONS **13,099** CITATIONS

Tang, S.-P. W., Spiro, T. G., Antanaitis, C., Moss, T. H., Holm, R. H., Herskovitz, T., & Mortensen, L. E. (1975) *Biochem. Biophys. Res. Commun. 62*, 1–6.

Wilson, E. B., Jr., Decius, J. C., & Cross, P. C. (1955) *Mo-lecular Vibrations; The Theory of Infrared and Raman Vibrational Spectra*, McGraw-Hill, New York.

York, J. L., & Bearden, A. J. (1970) *Biochemistry 9*, 4549–4554.

# Resonance Raman Examination of Axial Ligand Bonding and Spin-State Equilibria in Metmyoglobin Hydroxide and Other Heme Derivatives[†]

Sanford A. Asher* and Todd M. Schuster

ABSTRACT: Resonance Raman spectra and excitation profiles have been obtained within the 5700–6300-Å absorption band of purified sperm whale metmyoglobin hydroxide ($Mb^{III}OH$) solutions. A large enhancement occurs for a Raman peak at 490 cm$^{-1}$ which is shown by isotopic substitution of $^{18}O$ for $^{16}O$ to be almost purely an Fe–O stretch. The Fe–O vibration in $Mb^{III}OH$ occurs 5 cm$^{-1}$ to lower energy than the corresponding vibration at 495 cm$^{-1}$ in human methemoglobin hydroxide ($Hb^{III}OH$) [Asher, S., Vickery, L., Schuster, T., & Sauer, K. (1977) *Biochemistry 16*, 5849], reflecting differences in ligand bonding between Mb(III) and Hb(III). A larger frequency difference (10 cm$^{-1}$) exists between $Mb^{III}F$ and $Hb^{III}F$ for the Fe–F stretch. We do not observe separate Fe–O or Fe–F stretches from the $\alpha$ and $\beta$ chains of either $Hb^{III}OH$ or $Hb^{III}F$. Excitation profile measurements for $Mb^{III}OH$ indicate that the 5700–6300-Å absorption band is composed of two separate absorption bands which result from a high- and a low-spin form of $Mb^{III}OH$. The spin-state-sensitive Raman band at 1608 cm$^{-1}$ reflects the high-spin species and has an excitation profile maximum at about 6000 Å while the low-spin Raman band occurs at 1644 cm$^{-1}$ and shows an excitation profile maximum at 5800 Å. The Fe–O stretch at 490 cm$^{-1}$ has an excitation profile maximum at about 6000 Å. The differences in frequency and Raman cross section between the Fe–X vibrations in $Mb^{III}X$ and $Hb^{III}X$ (X = OH$^-$, F$^-$) can be related to increases in the out-of-plane iron distance for the high-spin species of $Mb^{III}X$. The shift in the 1644-cm$^{-1}$ $Mb^{III}OH$ low-spin-state Raman band indicative of the heme core size to 1636 cm$^{-1}$ in $Hb^{III}OH$ indicates a larger heme core size in $Hb^{III}OH$. Raman frequency shifts are used to estimate differences in bond strain energies between $Mb^{III}X$ and $Hb^{III}X$ (X = OH$^-$, F$^-$). Previous resonance Raman excitation profile data can be interpreted in terms of separate contributions from different spin-state species.

Although the heme geometries and tertiary protein structures of the subunits of hemoglobin and of myoglobin are qualitatively similar, some important differences in functional properties result from differences in the detailed heme geometry. These differences in heme geometry are apparent from the recent X-ray results (Takano, 1977a,b; Ladner et al., 1977) indicating that the iron in metmyoglobin derivatives lies farther from the heme plane than in the corresponding methemoglobin derivatives. This may account for the lower ligand affinities of myoglobin compared to those of hemoglobin in the oxy quarternary form (Antonini & Brunori, 1971) and for the increased magnetic susceptibility of metmyoglobin derivatives compared to those of methemoglobin (George et al., 1964; Iizuka & Kotani, 1969a,b).

Some derivatives of metmyoglobin [Mb(III)][1] and methemoglobin [Hb(III)] such as the azide and hydroxide complexes have magnetic susceptibilities at room temperature intermediate between those of a high-spin iron and those of a low-spin iron (Smith & Williams, 1968; Beetlestone & George, 1964). From the temperature dependence of the susceptibilities, it appears that these derivatives are in a thermal spin-state equilibrium due to the small energy difference between the high- and low-spin species [for a review, see Iizuka & Yonetani (1970)]. The exact energy difference depends on the detailed protein structure. For example, small changes in the spin-state equilibrium of some methemoglobin derivatives can be induced by addition of allosteric effectors which switch the quaternary structure of the hemoglobin tetramer (Perutz et al., 1974, 1978; Messana et al., 1978). However, the differences in tertiary protein structure between myoglobin and hemoglobin result in considerably larger spin-state differences than those which are produced in hemoglobin by effectors. For example, the hydroxide derivative of metmyoglobin is 70% high spin at room temperature while the corresponding derivative of methemoglobin is only 45% high spin (Beetlestone & George, 1964; George et al., 1964; Yonetani et al., 1971).

Since resonance Raman spectroscopy permits the selective observation of those heme vibrations which are vibronically active in the resonant electronic transition [for recent reviews see Warshel (1977a) and Yu (1977)], we have used this method to correlate changes in protein structure with changes in the spin-state equilibrium and the heme geometry of various Mb(III) and Hb(III) derivatives (Asher & Schuster, 1979). The resonance Raman technique may be utilized to examine environmentally sensitive heme vibrations such as the iron-axial ligand stretches (Kincaid et al., 1979a,b; Desbois et al., 1978, 1979; Chottard & Mansuy, 1977; Asher et al., 1977; Asher, 1976; Brunner, 1974) and other vibrational modes

[1] Abbreviations used: Mb(III), metmyoglobin; Hb(III), methemoglobin; $Fe^{III}POR$, ferric porphyrin; $R_{ct-N}$, distance between the center of the porphyrin and the pyrrole nitrogens; Fe–N$_e$, iron–proximal histidine bond; Hepes, 4-(2-hydroxyethyl)-1-piperazineethanesulfonic acid; InsP$_6$, inositol hexaphosphate.

which accurately reflect the spin state of the iron and the distance from the center of the heme to the pyrrole nitrogens (Spaulding et al., 1975; Huong & Pommier, 1977; Kitagawa et al., 1976). Simultaneous enhancement of different heme spin-state species can occur for those heme proteins existing in a spin-state equilibrium (Strekas & Spiro, 1974) provided that each of the individual species is in resonance. Excitation profiles of vibrational modes resulting from different spin-state species can be utilized to assign heme electronic transitions (Asher, 1976; Asher et al., 1977) and to relate these electronic transitions with individual spin-state species.

In this study we have examined the Fe–O axial ligand stretches in $Hb^{III}OH$ and $Mb^{III}OH$ and have correlated differences in spin-state equilibria with changes in the Fe–O stretching frequencies and heme geometries. We have observed the presence of a high- and low-spin species of both $Mb^{III}OH$ and $Hb^{III}OH$ which have different absorption spectra. In view of these results, we reinterpret previous Raman data of various Mb(III) and Hb(III) derivatives.

Experimental Section

The major component of human hemoglobin, $A_o$, was purified as oxyhemoglobin by the method of Williams & Tsay (1973). Methemoglobin was prepared by oxidation of hemoglobin with excess potassium ferricyanide, followed by extensive dialysis against doubly distilled water, and stored as 3% solutions in liquid $N_2$. Sperm whale myoglobin was obtained in the lyophilized met form from Miles-Seravac (batch 15). It was purified on a CM-50-Sephadex column resin according to the method of Hapner et al. (1968). The principal Mb component was used for the present studies. Fluorescence measurements by Dr. M. Sayare showed that the unpurified material exhibited several emission maxima which were removed by this purification. We used fraction 4 and stored it as the salt-free lyophilized powder. The myoglobin hydroxide and aquo complexes were prepared by dissolving the lyophilized purified protein in a buffer solution near to the desired pH value and then adjusting the pH to the final value by slowly titrating either with NaOH or HCl by using rapid stirring. $Mb^{III}F$ solutions were prepared by dissolving the lyophilized Mb(III) in a buffer solution containing 0.5 M NaF. All of the Hb(III) and Mb(III) solutions were filtered through extensively washed 1.2-$\mu$m pore size Millipore filters. Hemoglobin solutions were prepared in the same manner. $H_2^{18}O$ was obtained from Bio-Rad Corp. (99.12 atom % $^{18}O$).

Heme concentrations were measured in a 2-mm cuvette in a Cary 14 or Cary 118 spectrophotometer using extinction coefficients of George et al. (1964). All of the Raman spectra were obtained within 12 h of sample preparation. The absorption spectra were monitored both before and after obtaining the Raman spectra to check for sample decomposition. No decomposition was detected during the Raman measurements. However, we did find that $Mb^{III}OH$ solutions kept above pH 10 for over 24 h at 5 °C showed numerous changes in their low-frequency resonance Raman spectra. These changes are independent of laser illumination and indicate caution must be exercised with solutions of Mb(III) at high pH.

Resonance Raman spectra were measured at room temperature (21 ± 2 °C) by using 90° scattering in a rotating cell (>500 rpm). The Raman spectra were measured by using a Raman spectrometer constructed at the Gordon McKay Laboratory. Spectra were obtained by using a Coherent Radiation 490 dye laser pumped by a Spectra-Physics 171 $Ar^+$ laser. The dye laser intensity was stabilized to better than 2% by a feedback circuit to the power supply which adjusts the $Ar^+$ laser

output in response to variations in the dye laser output. The scattered light was collected by achromatic lenses, passed through a polarization scrambler, and focused onto a Spex 1400-II double monochromator equipped with a thermoelectrically cooled RCA C31034A-02 photomultiplier (PMT). The light incident on the PMT was focused onto the photocathode by a quartz lens situated between the PMT and the exit slit of the monochromator. The PMT output was fed into a PAR Model 1109 and Model 1121 photon counter and amplifier discriminator.

The photon counter and a stepping motor mounted on the monochromator are interfaced to a Declab 11/03 computer (Digital Equipment) which accumulates the data and controls the monochromator. The relative spectral efficiency of the Raman spectrometer was calibrated by using a standard intensity lamp (Ortec Corp.). All of the Raman spectra and excitation profiles were digitally normalized to the spectrometer efficiency profile. The spectra were also normalized for self-absorption (Strekas et al., 1974). We estimate that the absolute Raman frequencies reported for nonoverlapping peaks to be accurate to ±2 $cm^{-1}$. The shifts in frequency of the iron–axial ligand stretching vibrations between Mb(III) and Hb(III) were measured more carefully and are accurate to ±1 $cm^{-1}$. Excitation profile intensity data were obtained for resolved Raman peaks by peak height or peak integration and then normalized to the internal standard. Base lines were assumed to be continuous and to vary linearly through the Raman peak. Both the peak-height and peak-integration techniques yielded identical results for isolated bands, and we estimate that the excitation profile intensity ratio measurements are accurate to ±10%. For the overlapping series of peaks in the 1500–1650-$cm^{-1}$ region of $Mb^{III}OH$, peak-height measurements were used and the base line was taken as a straight line between the intensity values at 1500 and 1670 $cm^{-1}$. Due to the complex series of at least eight overlapping bands in this region and the rough estimates required for the base lines, excitation profile data between 1500 and 1670 $cm^{-1}$ should only be considered as qualitative.

Results

Figure 1 shows the resonance Raman spectra of the $^{16}OH$ and $^{18}OH$ derivatives of Mb(III). These spectra were excited within the long-wavelength absorption band maximum which is essentially flat from ca. 5800 to 6000 Å (Figure 3). The bands at 983 $cm^{-1}$ in all of the Raman spectra are due to sulfate added as an internal standard. The two spectra in Figure 1 are essentially identical except for the shift of the 490-$cm^{-1}$ peak from $Mb^{III 16}OH$ to 468 $cm^{-1}$ in $Mb^{III 18}OH$. We assign the 490-$cm^{-1}$ peak from $Mb^{III}OH$ to the Fe–O axial ligand stretch on the basis of the 22-$cm^{-1}$ isotopic shift, since this is exactly the shift expected by using a harmonic oscillator approximation for a pure Fe–O diatomic stretch. The observed isotopic shift and the assignment of the Fe–O stretch in $Mb^{III}OH$ agree with the recent results of Desbois et al. (1978, 1979).

Figure 2 compares the resonance Raman spectrum excited at 5998.5 Å of $Mb^{III}OH$ with that of $Hb^{III}OH$. The peak appearing at 495 $cm^{-1}$ previously shown by isotopic substitution to correspond to the Fe–O diatomic stretch of $Hb^{III}OH$ (Asher et al., 1977) occurs 5 ± 1 $cm^{-1}$ to higher frequency from that of $Mb^{III}OH$. The 2-$cm^{-1}$ difference in the frequency of the Fe–O stretch we measure for $Hb^{III}OH$ (495 $cm^{-1}$) compared to that previously measured by Asher et al. (1977) (497 $cm^{-1}$) is within the estimated accuracy of our earlier measurement. It should be noted that only one peak is observed for the Fe–O stretches in the $\alpha$ and $\beta$ subunits of $Hb^{III}OH$, indicating that
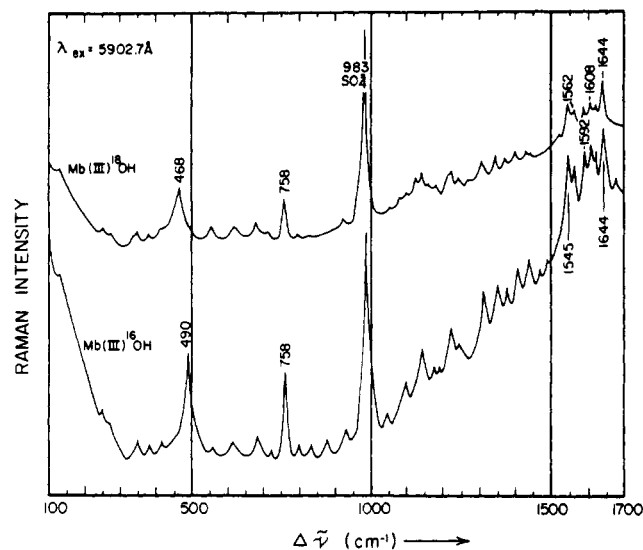
FIGURE 1: Resonance Raman spectra of Mb$^{III18}$OH and Mb$^{III16}$OH excited at 5902.7 Å. Mb$^{III18}$OH: heme concentration = 0.3 mM heme; 0.25 M Na$_2$SO$_4$; 0.025 M borate buffer; pH 10.82; two scans. Mb$^{III16}$OH: heme concentration = 0.31 mM heme; 0.25 M Na$_2$SO$_4$; 0.025 M borate buffer; pH 10.18; one scan. Laser power = 0.3 W; integration time = 1 s; average slit width = 2.8 cm$^{-1}$.
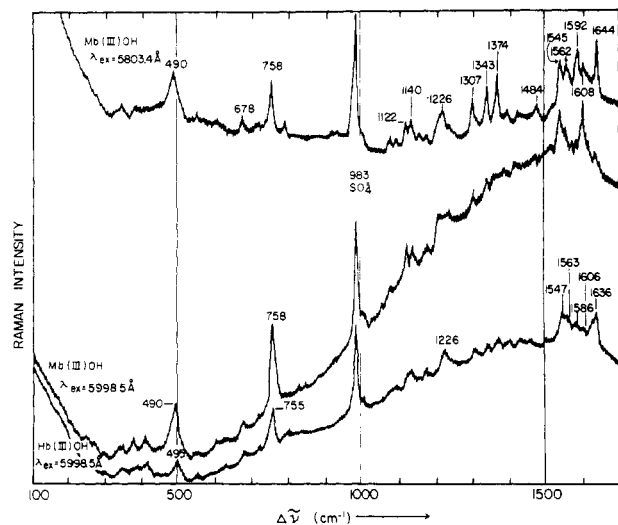


FIGURE 2: Resonance Raman spectra of Mb$^{III}$OH and Hb$^{III}$OH. Hb$^{III}$OH: $\lambda_{ex}$ = 5998.5 Å; heme concentration = 0.36 mM; 0.2 M Na$_2$SO$_4$; 0.02 M borate buffer; pH 10.62; nine scans; laser power = 0.3 W. Mb$^{III}$OH: heme concentration = 0.31 mM; 0.25 M Na$_2$SO$_4$; 0.025 M borate buffer; pH 10.18. $\lambda_{ex}$ = 5998.5 Å; laser power = 0.3 W; integration time = 1 s; average slit width = 2.7 cm$^{-1}$; one scan. $\lambda_{ex}$ = 5803.4; laser power = 0.4 W; integration time = 2 s; average slit width = 2.9 cm$^{-1}$; two scans.

the Fe–O stretches of the $\alpha$ and $\beta$ subunits have similar frequencies or that the Fe–O stretch is selectively enhanced only in the $\alpha$ or $\beta$ chains.

The resonance Raman spectra of Mb$^{III}$OH and Hb$^{III}$OH shown in Figures 1 and 2 displaying a complex series of overlapping peaks in the 1500-1700-cm$^{-1}$ region are somewhat similar to spectra obtained earlier by Ozaki et al. (1976) using 4880-Å excitation. Most of the features between 1500 and 1700 cm$^{-1}$ are assignable to those porphyrin macrocyclic vibrational modes whose frequencies are dependent upon the spin state of the heme iron (Spiro & Burke, 1976; Spiro, 1975; Kitagawa et al., 1976). The depolarized peak at 1644 cm$^{-1}$ and the anomalously polarized peaks at 1592 cm$^{-1}$ in Mb$^{III}$OH and at 1636 and 1586 cm$^{-1}$ for Hb$^{III}$OH result from low-spin iron species while the depolarized peaks at 1608 and 1545 cm$^{-1}$
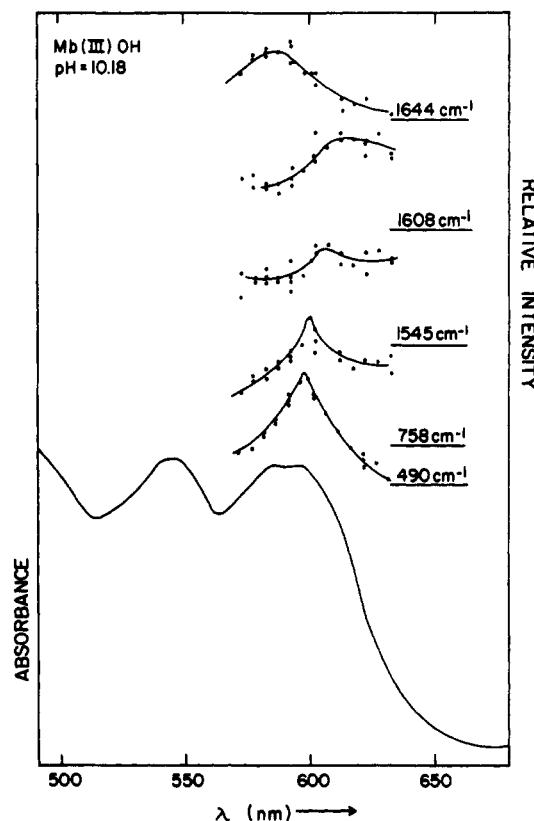


FIGURE 3: Excitation profiles and absorption spectrum of Mb$^{III}$OH. The excitation profiles of the 1545-, 1608-, and 1644-cm$^{-1}$ peaks should be regarded as qualitative due to the difficulties in resolving the overlapping peaks.

in Mb$^{III}$OH and 1606 and 1547 cm$^{-1}$ for Hb$^{III}$OH are due to high-spin iron species. The simultaneous appearance of vibrational modes characteristic of both high- and low-spin species occurs because both Mb$^{III}$OH and Hb$^{III}$OH exist in a thermal spin-state equilibrium at room temperature with 55:45 and 30:70 mixtures of low to high spin in Hb$^{III}$OH and Mb$^{III}$OH, respectively (Beetlestone & George, 1964; George et al., 1964).

In Mb$^{III}$OH the relative intensities of the peaks between 1500 and 1700 cm$^{-1}$ change dramatically as a function of the excitation wavelength. Excitation at wavelengths greater than 6000 Å leads to a simplification of the 1500-1700-cm$^{-1}$ region of the Raman spectra; only the 1545- and 1608-cm$^{-1}$ peaks are significantly enhanced (Figure 2). In contrast, excitation toward the short-wavelength side of the 5800-6000-Å absorption band shown in Figure 3 results in an increased intensity for Raman bands at 1644, 1592, and 1562 cm$^{-1}$ (Figures 1 and 2). It should be noted that, due to the overlapping peaks (at least eight) in the 1500-1700-cm$^{-1}$ frequency region, the errors for some of the peak frequencies quoted could be as large as ±3 cm$^{-1}$.

Figure 3 compares the excitation profiles of some of the Mb$^{III}$OH Raman peaks with the absorption spectrum. Both the 490-cm$^{-1}$ Fe–O stretch and the 758-cm$^{-1}$ porphyrin macrocycle peak show excitation profile maxima at about 6000 Å, at the long-wavelength edge of the 5800-6000-Å absorption band maximum. The excitation profile of the 758-cm$^{-1}$ peak shows broad shoulders, indicating enhancement everywhere within this absorption band, but a maximum is clearly visible at ca. 6000 Å. Although there are indications that small changes in width and frequency of this peak occur as a function of excitation wavelength, we did not characterize this fully. The 490-cm$^{-1}$ Fe–O stretch shows a clear and almost symme-
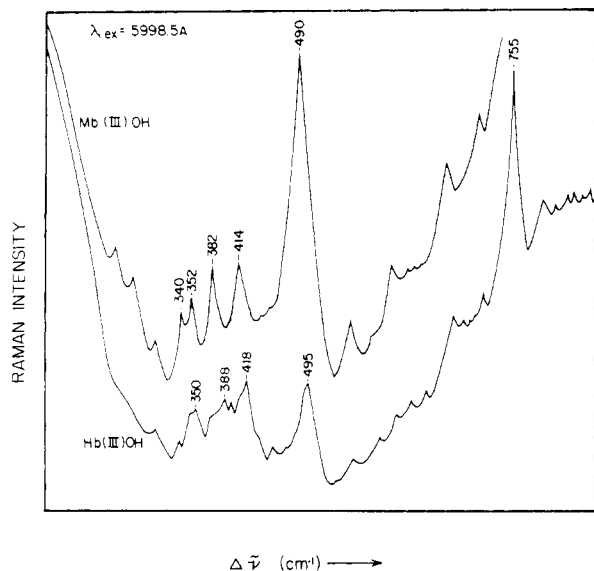
FIGURE 4: Low-frequency region of the resonance Raman spectra of Hb$^{III}$OH and Mb$^{III}$OH; $\lambda_{ex}$ = 5998.5 Å. Conditions are as described in Figure 2.



FIGURE 5: Resonance Raman spectrum of Mb$^{III}$F. $\lambda_{ex}$ = 5999.7 Å; heme concentration = 0.27 mM; 0.2 M Na$_2$SO$_4$; 0.1 M Hepes buffer; 0.5 M NaF; pH 6.77; three scans; laser power = 0.5 W; integration time = 1 s; average slit width = 4.1 cm$^{-1}$.

tric excitation profile with a maximum at 6000 Å indicating that it is in resonance with a component of the absorption spectrum at ca. 6000 Å.

The 1644-cm$^{-1}$ band which is the most clearly resolved peak between 1500 and 1700 cm$^{-1}$ shows a clear excitation profile maximum at about 5800 Å, while the peaks at 1608 and 1545 cm$^{-1}$ are enhanced by a component at 6000 Å in the absorption spectrum. The selective enhancement of the 1608- and 1545-cm$^{-1}$ peaks at the long-wavelength side of the 5800–6000 absorption band maximum is clearly evident in the 5998.5-Å excited resonance Raman spectrum of Mb$^{III}$OH shown in Figure 2. However, the overlap of numerous bands in this spectral region results in uncertainties for the base-line and peak-height values, leading to somewhat broad excitation profiles.

Figure 4 shows the low-frequency resonance Raman spectra of Hb$^{III}$OH and Mb$^{III}$OH excited at 6000 Å. Although the features are relatively weak, a doublet can be observed at 340 and 352 cm$^{-1}$ in Mb$^{III}$OH which presumably corresponds to the broad 352-cm$^{-1}$ peak in Hb$^{III}$OH. The 382- and 414-cm$^{-1}$ features in Mb$^{III}$OH appear to shift to 389 and 418 cm$^{-1}$ in Hb$^{III}$OH. The low-frequency Raman spectrum of Mb$^{III}$OH excited at ca. 6000 Å is qualitatively similar to the spectrum obtained by Desbois et al. (1978, 1979), excited near the Soret band. Some of these features could correspond to heme macrocycle vibrations containing contributions from Fe–proximal nitrogen stretches while others may contain a contribution from the Fe–proximal histidine stretch (Kincaid et al., 1979a; Desbois et al., 1978, 1979).

Figure 5 shows the resonance Raman spectrum of Mb$^{III}$F excited at 5999.7 Å near the maximum of its ca. 6100-Å charge-transfer absorption band. The doublet appearing at 461 and 422 cm$^{-1}$ correlates with the doublet observed by Asher et al. (1977) for Hb$^{III}$F which they assigned to Fe–F stretches; the lower frequency component occurring at 443 cm$^{-1}$ in Hb$^{III}$F was assigned to an Fe–F stretch lowered in frequency due to hydrogen bonding with a water molecule in some of the heme pockets while the higher frequency component at 471 cm$^{-1}$ was assigned to an unperturbed Fe–F stretch. The decrease in frequency for the Fe–F stretches in Mb$^{III}$F from that in Hb$^{III}$F is in the same direction as the frequency shift observed for the Fe–O stretch between Hb$^{III}$OH and
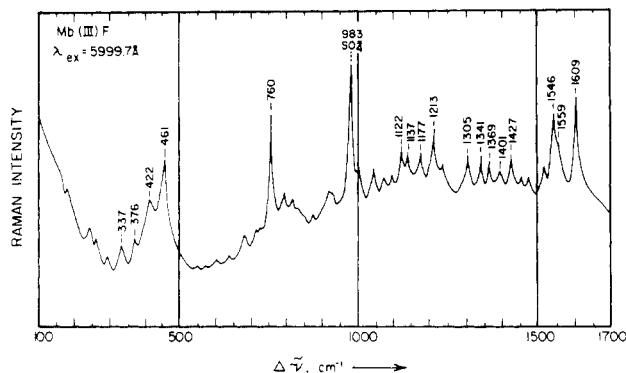
Mb$^{III}$OH (Figure 2). However, the frequency shift is much larger for the fluoride derivatives since the unperturbed Fe–F stretch shifts by 10 cm$^{-1}$ while the hydrogen-bonded Fe–F stretch shifts by 20 cm$^{-1}$. Some of the other Mb$^{III}$F Raman peaks are shifted in frequency from that observed in Hb$^{III}$F (Asher et al., 1977). However, these shifts are smaller than those for the Fe–F stretches. The frequencies of the 760- and 1610-cm$^{-1}$ peaks are essentially identical for Mb$^{III}$F and Hb$^{III}$F.

## Discussion

*Correlation of Axial Ligand Enhancement and Heme Spin State.* Resonance Raman excitation within those in-plane $\pi$ → $\pi^*$ electronic transitions of the heme macrocycle which result in the visible and near-UV $\alpha$, $\beta$, and Soret absorption bands mainly enhances heme macrocyclic vibrational modes. Iron–axial ligand modes show little enhancement within these absorption bands because of weak coupling of the iron and the axial ligand molecular orbitals to the $\pi$ orbitals of the porphyrin. However, significant enhancement of iron–axial ligand modes can occur upon excitation within heme and metalloporphyrin charge-transfer transitions (Asher & Sauer, 1976; Asher et al., 1977).

The presence of charge-transfer electronic transitions in hemes is reflected by additional absorption bands or by a broadening of the $\alpha$, $\beta$, or Soret bands. The magnitude of the charge-transfer contribution to the absorption spectra of heme proteins is related to the energy difference between the metal d and porphyrin $\pi$ orbitals and to the identity of the fifth and sixth axial ligands. This dependence is clearly evident in Hb(III) and Mb(III) derivatives. For example, the fluoride derivatives (high spin) have intense charge-transfer bands at ca. 6000 Å, while the azides (mixed spin) have much weaker bands at 6400 Å. In contrast, the cyanide derivatives (low spin) appear to have completely normal spectra showing just the $\alpha$ and $\beta$ and Soret bands (Smith & Williams, 1970; Eaton & Hochstrasser, 1968; Asher et al., 1977).

There appears to be a direct correlation between the spin state of the heme derivatives and the intensity of a charge-transfer transition at ca. 6000 Å; the intensity of this band has been correlated with increasing magnetic susceptibility (Smith & Williams, 1968). Indeed, George et al. (1961, 1964) from magnetic susceptibility and absorption studies of the fluoride and hydroxide derivatives of a number of heme proteins were able to calculate the separate absorption spectra of both the high- and low-spin species; the long-wavelength absorption maximum of the low-spin species occurs at ca. 5800 Å, while in the high-spin species it occurs at ca. 6000 Å.

These empirical correlations of the 6000-Å charge-transfer absorption band in $Mb^{III}OH$ with the high-spin species and the 5800-Å absorption band with the low-spin species are confirmed by the resonance Raman spectra shown in Figures 1 and 2 and the excitation profiles shown in Figure 3. These data demonstrate the simultaneous enhancement of the Fe–O stretch and the 1545- and 1608-cm$^{-1}$ Raman peaks which have been assigned to a high-spin heme (Kitagawa et al., 1976; Spiro & Burke, 1976; Spiro, 1975) within a component of the absorption spectrum centered at ca. 6000 Å. Excitation within the component of the absorption spectrum at 5800 Å results in enhancement of the 1586- and 1644-cm$^{-1}$ Raman peaks diagnostic of low-spin heme species. The lack of enhancement of the Fe–O stretch within the absorption component of the low-spin heme species indicates little or no charge-transfer contribution; the 5800-Å absorption band may simply derive from the $\alpha$ band of low-spin $Mb^{III}OH$.

The clearly observed correlation in $Mb^{III}OH$ between the enhancement of high-spin-state Raman vibrations and the enhancement of the axial ligand stretch in the 6000-Å absorption band appears also to be true for other Mb(III) and Hb(III) derivatives. High-spin-state Raman peaks at ca. 1608 and 1550 cm$^{-1}$ are observed for $Hb^{III}OH$ (Figure 2) and for $Hb^{III}N_3$ (Asher et al., 1977) upon excitation within the 6000–6400-Å absorption bands. Indeed, the ca. 1550- and 1608-cm$^{-1}$ peaks are the dominant features upon excitation on the long-wavelength side of the 6000- and 6400-Å absorption bands of $Hb^{III}OH$ and $Hb^{III}N_3$.

Since $Hb^{III}OH$ and $Hb^{III}N_3$ each exhibit a thermal spin-state equilibrium, it is probable that the iron–axial modes observed by Asher et al. (1977) derived from only the high-spin species of each mixed-spin derivative. It should be noted that spectrally distinct high- and low-spin species are also observed in IR studies of methemoglobin(III) and metmyoglobin(III) azide (Alben & Fager, 1972; McCoy & Caughey, 1970; Perutz et al., 1978). The internal azide vibrational frequencies of the low-spin species are shifted 25 cm$^{-1}$ below that of free azide in solution. In contrast, the high-spin species show a shift of only a few reciprocal centimeters, indicating that the iron–azide binding is predominantly ionic.

Recently, Desbois et al. (1978, 1979) reported on the iron–axial ligand modes observed in the resonance Raman spectra of various Mb(III) derivatives excited near the Soret band and assigned a number of iron–axial ligand modes. The assignments of the Fe–O and Fe–F vibrations are consistent with those presented here and by Asher et al. (1977). However, on the basis of a 16-cm$^{-1}$ isotope shift in $Mb^{III}N_3$ upon substitution of [$^{15}$N]azide, Desbois et al. assigned a 570-cm$^{-1}$ Raman feature to the Fe–azide stretch. In contrast, Asher et al. assigned a 413-cm$^{-1}$ feature to the Fe–azide stretch on the basis of its selective enhancement within the $Hb^{III}N_3$ charge-transfer band and its proximity to the 421-cm$^{-1}$ Fe–azide stretch observed in the IR spectrum of iron(III) octaethylporphyrin azide (Ogoshi et al., 1973). Although the results of Desbois et al. appear to be in conflict with those of Asher et al., the differences could be explained by the fact that Asher et al. and Desbois et al. assign the Fe–azide stretches in different spin-state species; Asher et al. were clearly observing the high-spin $Hb^{III}N_3$ species while Desbois et al. may have been selectively observing the low-spin species. Both high- and low-spin azide ligated Hb(III) and Mb(III) species are observed by using IR spectroscopy (Alben & Fager, 1972; McCoy & Caughey, 1970; Perutz et al., 1978). Furthermore, the attempt by Desbois to observe an isotope shift for the lower concentration high-spin $Mb^{III}N_3$ species [ca. 20%; Smith &

Table I: Relative Raman Cross Sections of High-Spin Axial Ligand Modes

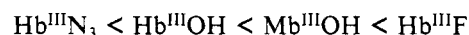| species | $\bar{\nu}$ (cm$^{-1}$) | % high-spin | Raman cross section[a] |
|---|---|---|---|
| $Hb^{III}F$ | 471, 443[b] | 97[c] | 1 |
| $Mb^{III}OH$ | 490 | 70[d] | 0.85 |
| $Hb^{III}OH$ | 495 | 45[e] | 0.26 |
| $Hb^{III}N_3$ | 413[b] | 10[f] | 0.25 |

[a] Raman cross sections measured at the maximum of the charge-transfer band are normalized to the concentration of the high-spin species. The cross section for $Hb^{III}F$ has been made equal to 1. [b] Asher et al. (1977). [c] Perutz et al. (1974). [d] Beetlestone & George (1964). [e] Yonetani et al. (1971). [f] Perutz et al. (1978).

Williams (1968)] would have been complicated by the presence of a 412-cm$^{-1}$ feature observed for all of their Soret excited myoglobin derivatives. Indeed, the 412-cm$^{-1}$ peak does show a -1.5-cm$^{-1}$ shift upon $^{15}$N substitutions (Desbois et al., 1979). The fact that the Fe–N (azide) stretch observed by Desbois et al. at 570 cm$^{-1}$ occurs at ca. 160 cm$^{-1}$ to higher frequency from the high-spin Fe–$N_3$ stretch observed in $Hb^{III}N_3$ (Asher et al., 1977) indicates an increased bond order in the low-spin ligated species. This increased bond order apparently correlates with a decreased frequency for the internal azide stretches in the low-spin azide complexes of Mb(III) and Hb(III) compared to those in the high-spin complexes (Alben & Fager, 1972; McCoy & Caughey, 1970; Perutz et al., 1978).

*Dependence of Axial Ligand Enhancement on Heme Geometry.* The relative intensities of the iron–axial ligand stretches vary dramatically between different Hb(III) and Mb(III) derivatives (Asher et al., 1977). If excitation occurs directly into the charge transfer band maxima of $Hb^{III}F$, $Mb^{III}F$, and $Mb^{III}OH$, the Fe–F and Fe–O stretches dominate the resonance Raman spectra. In contrast, the intensities of the iron–axial ligand stretches are much weaker in $Mb^{III}OH$ and $Hb^{III}N_3$. The relative Raman cross sections of the iron–axial ligand stretches in different Hb(III) and Mb(III) derivatives can be calculated from the ratio of the intensities of the iron–axial ligand stretches to the internal sulfate standard, by normalizing with respect to heme, $SO_4$, and high-spin concentration, provided the intensity measurements are made at the excitation profile maxima of each of the Fe–axial ligand Raman modes.

As the concentration of the high-spin species in the thermal spin-state equilibrium increases in the series

$$Hb^{III}N_3 < Hb^{III}OH < Mb^{III}OH < Hb^{III}F$$

the measured Raman cross section of the axial ligand mode also increases (see Table I).

It can be seen in Table I that there is not a linear correlation between the magnitude of the Raman cross section and the concentration of the high-spin species. However, this is not surprising since the cross section is dependent on numerous factors including vibronic interactions within the heme electronic transitions and Franck–Condon overlap factors which are determined by the detailed heme geometry as influenced by the globin. It should be noted that there is a threefold difference in the Raman cross section between $Mb^{III}OH$ and $Hb^{III}OH$.

Since the intense, long-wavelength charge-transfer bands of the $F^-$ and $OH^-$ derivatives of Hb(III) and Mb(III) occur at essentially the same wavelength, they probably derive from almost identical heme molecular orbitals with similar contributions from the atomic and molecular orbitals of the Fe, axial ligands, and porphyrin. Indeed, George et al. (1961, 1964) calculate that the extinction coefficient of the pure high-spin

6000-Å absorption band of Mb$^{III}$OH is only 10% greater than that of Hb$^{III}$OH. Thus, the threefold enhancement in the cross section of the Fe–O stretch in Mb$^{III}$OH over that in Hb$^{III}$OH must derive from a subtle geometric and electronic difference which is magnified by the resonance Raman process.

An examination of the quantum mechanical expression for resonance Raman scattering can rationalize the dramatic increase in the Raman cross section for the Fe–O stretch if one assumes small differences in the iron out-of-plane distances between Mb$^{III}$OH and Hb$^{III}$OH. In the Albrecht (1971) formulation for resonance Raman scattering, the intensity of scattering derives from two terms labeled A and B. The B-term enhancement results from vibronic interactions which couple different electronic transitions while the A-term enhancement results from favorable Franck–Condon overlap factors and is especially important for polarized, totally symmetric vibrations such as the iron–axial ligand stretches.

If A-term enhancement of the Fe–O stretch were due to the out-of-plane component of the heme electronic transition, it would have a fourth-power dependence upon the projection of the dipole transition moment, $\langle s|er|g \rangle$, normal to the heme plane, where $g$ and $s$ label the ground and excited states and $er$ is the electric dipole moment operator.

If the out-of-plane component of the transition moment scales with the out-of-plane iron distance $d$, then the ratio, $R$, of the Raman cross sections of Mb$^{III}$OH to Hb$^{III}$OH would be expected to be given by

$$R \simeq (d_{Mb}/d_{HB})^4 = 3$$

Since there are no X-ray structural data available for Hb$^{III}$OH and Mb$^{III}$OH, we cannot directly test this relationship. However, this value of $R = 3$ (see Table I) is consistent with the recent X-ray diffraction data of the aquo derivatives of Mb(III) and Hb(III); the heme iron appears to lie farther from the pyrrole nitrogen plane in Mb(III) than in Hb(III). Takano (1977a) reports that the iron in sperm whale aquo-Mb(III) lies 0.4 Å from the mean heme plane and 0.27 Å from the plane defined by the four pyrrole nitrogens. In contrast, Ladner et al. (1977) could not resolve any doming of the pyrrole nitrogens in horse Hb(III) but found that the iron atoms in the $\alpha$ and $\beta$ subunits were 0.07 and 0.21 Å from the heme plane, respectively.

Perutz et al. (1978) have presented evidence that most of the high-spin species in Hb$^{III}$N$_3$ reside in the $\beta$-chain hemes. Since iron–axial ligand modes are only enhanced within the high-spin heme species, the Fe–N (azide) stretches previously observed must have derived solely from the $\beta$ subunits. If the localization of the high-spin species in Hb$^{III}$OH is also mainly in the $\beta$ subunits, then the X-ray data of Mb$^{III}$OH should be compared to that of the $\beta$ subunits in aquo-Hb(III). The assumption that the iron out-of-plane distances are the same for the aquo and hydroxy derivatives is not unreasonable since the X-ray difference Fourier diffraction pattern between horse aquo-Hb(III) and Hb(III)F is featureless around the hemes (Deatherage et al., 1976). Thus

$$R = (0.27 \text{ Å}/0.21 \text{ Å})^4 = 2.7$$

which is close to the measured ratio of 3 (Table I). If the in-plane component of the electronic transition is conserved between Mb$^{III}$OH and Hb$^{III}$OH, the small increase in the out-of-plane component would result in only a small increase in the extinction coefficient.

*Differences in Heme Geometry between High-Spin Methemoglobin and Metmyoglobin Hydroxide and Fluoride.* We assume that the 5-cm$^{-1}$ decrease in the frequency of the Fe–O stretch in Mb$^{III}$OH compared to that in Hb$^{III}$OH is due to an increased out-of-plane distance for the iron atom in high-spin Mb$^{III}$OH over that in Hb$^{III}$OH. The origin of the frequency shift would be due to a stretching of the Fe–O bond due to nonbonding interactions with the van der Waals radii of the pyrrole nitrogens; the Fe–O linkage cannot rigidly follow the iron movement to the proximal side of the heme plane. The resulting elongation of the bond results in a decreased bond order and force constant. The force constant decreases from $1.79 \times 10^{-3}$ dyn/Å in Hb$^{III}$OH to $1.76 \times 10^{-3}$ dyn/Å in Mb$^{III}$OH. This change in the force constant of the Fe–O stretch between Hb$^{III}$OH and Mb$^{III}$OH appears to result primarily from geometric changes at the heme core and not in the heme macrocycle since the frequencies of those Raman peaks sensitive to the heme macrocycle geometry in the high-spin species of Hb$^{III}$OH and Mb$^{III}$OH are essentially identical.

We attempted to directly examine differences in hydroxide binding in Mb(III) and Hb(III) by examining differences in the anharmonicity of the Fe–O stretches evidenced by shifts in the overtone frequencies. Unfortunately, the intensities of the overtones were too small to observe. However, information about the changes in the high-spin heme geometries can be obtained by examining the corresponding high-spin fluoride complexes.

Previously, in a comparison of the Fe–F stretch between iron(III) porphyrin fluorides (Fe$^{III}$PORF) and Hb$^{III}$F, Asher et al. (1977) noted that the Fe–F stretch shifts by 120 cm$^{-1}$ to lower frequency in Hb$^{III}$F (471 cm$^{-1}$) compared with that of the non-protein-bound iron(III) porphyrin fluoride complexes [590 cm$^{-1}$; Kincaid & Nakamoto (1976), Spiro & Burke (1976), and Ogoshi et al. (1973)]. The 120-cm$^{-1}$ shift between Fe$^{III}$PORF and Hb$^{III}$F corresponds to a decrease in the force constant of the Fe–F stretch from $2.91 \times 10^{-3}$ to $1.85 \times 10^{-3}$ dyn/Å. Asher et al. estimated that a 36% decrease in the frequency of the non-hydrogen-bonded Fe–F stretch results from a 15% elongation of the Fe–F bond due to the steric constraints imposed by the pyrrole nitrogen [see Note Added in Proof in Asher et al. (1977)].

It has been shown that azide is ionically bound in the high-spin azide derivatives of Hb(III) and Mb(III) (McCoy & Caughey, 1970; Alben & Fager, 1972; Perutz et al., 1978). Since the binding of the F$^-$ and OH$^-$ axial ligands to the iron is probably similar and ionic, we can approximate the relationship between the force constant of the diatomic Fe–axial ligand mode and the equilibrium bond length by assuming a potential function for the vibration with a Coulombic attractive term.

The vibrational potential function, $U$, for the Fe–axial ligand vibration can be approximated as

$$U = \frac{A}{r^n} + \frac{Z_1 Z_2}{r} \tag{1}$$

where the first term accounts for the repulsive interaction of the axial ligand with the heme and the iron and assumes that this repulsive interaction occurs along the bond axis and that $r$ in both the repulsive and attractive terms represents the distance between the axial ligand and the iron. $Z_1$ and $Z_2$ are the effective charges of the sixth axial ligand and the iron, respectively. The factor $A$ defines the magnitude of the repulsion. As will be shown later, the exact form of the repulsive term is not essential to our argument.

The equilibrium bond length is obtained by minimizing the potential. If $Z_1 = -e$ and $Z_2 = e$, where $e$ is the charge on an electron, then

$$\frac{\partial U}{\partial r} = 0 = -nAr^{-(n+1)} + e^2 r^{-2} \tag{2}$$

$$r_e = \left(\frac{nA}{e^2}\right)^{1/(n-1)} \tag{3}$$

The force constant $k$ is the second derivative of the potential evaluated at the equilibrium position, $r_e$:

$$k = (n - 1)e^2 r_e^{-3} \tag{4}$$

Provided that $n > 1$, the repulsive potential function has a minimum as evidenced by a positive value for $k$. For different heme proteins and iron porphyrins, changes in the force constant and the resulting Raman frequency, $\nu$, for a particular axial ligand can be related to differences in the equilibrium Fe–axial ligand bond lengths by eq 4. If $n$ is constant, then

$$\frac{k_1}{k_2} = \left(\frac{\nu_1}{\nu_2}\right)^2 = \frac{n_1 - 1}{n_2 - 1}\left(\frac{r_2}{r_1}\right)^3 \sim \left(\frac{r_2}{r_1}\right)^3 \tag{5}$$

For the case of two heme proteins which differ because the heme iron of one is constrained to lie slightly farther to the proximal side of the heme plane, this expression requires that the increased axial ligand–pyrrole nitrogen interaction is reflected only by an increase in $A$ with no change in $n$. If we use eq 5 to estimate the change in $r_e$ between Fe(III)PORF with $k_1 = 2.91 \times 10^{-3}$ dyn/Å and $r = 1.97$ Å (sum of ionic radii) and Hb(III)F with $k_2 = 1.85 \times 10^{-3}$ dyn/Å, the Fe–F bond length would be $r_2 = 2.29$ Å for $Hb^{III}F$. This value is the same as that suggested by Asher et al. (1977) on the basis of the bond elongation expected from nonbonded interactions of the ionic radius of the $F^-$ with the van der Waals radii of the pyrrole nitrogens.

The value of the exponent $n$ in the repulsion potential can be estimated by using eq 4. By use of the force constants and bond distances for $Hb^{III}F$ or $Fe^{III}PORF$, $n = 10.7$, compared with the value of $n = 12$ appearing in the Lennard–Jones potential (Kittel, 1971). If the Fe–O bond length in $Hb^{III}OH$ were 1.84 Å as in the methoxy complex of iron(III) mesoporphyrin IX dimethyl ester (Hoard et al., 1965), the 5-cm$^{-1}$ decrease in the Fe–O stretching frequency in $Mb^{III}OH$ from that in $Hb^{III}OH$ indicates an Fe–O bond elongation of 0.013 Å for $Mb^{III}OH$. Alternatively, if the Fe–O bond length were 2.2 Å as reported for aquohydroxy iron(III) tetraphenylporphine [Fleisher et al. (1964); however, see Hoard et al. (1965)], the elongation would be 0.015 Å. This elongation of the bond presumably results from an increased displacement of the iron atom toward the proximal histidine side of the heme plane in $Mb^{III}OH$ compared with that in $Hb^{III}OH$.

Asher et al. (1977) assigned the Fe–F stretch in $Hb^{III}F$ to a doublet occurring at 471 and 443 cm$^{-1}$. The 443-cm$^{-1}$ peak was assigned to an Fe–F stretch which was hydrogen bonded to a water molecule in some of the heme pockets while the 471-cm$^{-1}$ peak was assigned to the unperturbed Fe–F stretch. They also noted the presence of this doublet in the resonance Raman spectrum of $Mb^{III}F$ excited within its 6000-Å charge-transfer band.

An examination of the corresponding Fe–F stretches in $Mb^{III}F$ (Figure 5) indicates that they occur at lower frequencies in $Mb^{III}F$ (461 and 422 cm$^{-1}$) than in $Hb^{III}F$ (471 and 443 cm$^{-1}$). These data indicate a decrease in the force constant of the non-hydrogen-bonded Fe–F stretch from $1.85 \times 10^{-3}$ dyn/Å in $Hb^{III}F$ to $1.77 \times 10^{-3}$ dyn/Å in $Mb^{III}F$ and suggest, using eq 5, an elongation of 0.05 Å for the Fe–F bond in Mb(III) over that in Hb(III). This increase in the Fe–F bond length for $Mb^{III}F$ is similar to the 0.06-Å increase observed by using X-ray diffraction for the out-of-plane iron distance in $Mb^{III}H_2O$ compared to that of $Hb^{III}H_2O$ (Takano, 1977a; Ladner et al., 1977) and correlates well with EPR measure-

Table II: Iron–Axial Ligand Force Constants and Calculated Bond Lengths and Stored Strain Energies

| species | $\nu^a$ (cm$^{-1}$) | force constant ($10^{-3}$ dyn/Å) | $r_{Fe-X}$ (Å) | strain energy (kcal/mol of heme) |
|---|---|---|---|---|
| $Hb^{III}OH$ | 495 | 1.79 | 1.840 | $c$ |
| $Mb^{III}OH$ | 490 | 1.76 | 1.853 | $c$ |
| $Fe^{III}PORF$ | 590$^b$ | 2.91 | 1.97 | 0.0 |
| $Hb^{III}F$ | 471 | 1.85 | 2.29 | 7.9 |
| $Mb^{III}F$ | 461 | 1.77 | 2.34 | 10.1 |

$^a$ Stretching frequency of Fe–X (X = OH$^-$, F$^-$). $^b$ This is taken as the average of values for various iron(III) porphyrin fluorides (Kincaid & Nakamoto, 1976; Spiro & Burke, 1976; Ogoshi et al., 1973). $^c$ See the text.

ments indicating a decrease in bonding from $Hb^{III}F$ to $Mb^{III}F$ (Morimoto & Kotani, 1966). The calculated iron–axial ligand bond distances are summarized in Table II.

We can estimate the strain energy stored in the Fe–F bond in $Hb^{III}F$ compared to that of $Fe^{III}PORF$ if we take the bond to be unstrained in the non-protein-bound heme:

$$E = \frac{1}{2}\int_{r_o}^{r_H} k(r - r_o)\, dr = \frac{(n - 1)e^2}{2}\int_{r_o}^{r_H}\frac{(r - r_o)\, dr}{r^3} = \frac{(n - 1)e^2}{4}\frac{(r_H - r_o)^2}{2 r_o r_H^2} \tag{6}$$

where $r_o$ and $r_H$ are the Fe–F bond lengths in $Fe^{III}PORF$ and $Hb^{III}F$, respectively. By use of $n = 10.7$, $r_o = 1.97$ Å, and $r_H = 2.29$ Å, $E = 5.5 \times 10^{-13}$ erg/mol or 7.9 kcal/mol of heme.

By use of eq 6, the strain energy present in the Fe–F bond in $Mb^{III}F$ compared to that in $Fe^{III}PORF$ is $7.5 \times 10^{-13}$ erg/mol or 10.1 kcal/mol of heme. Thus, there appears to be an increase of 2.2 kcal for the strain energy stored in the Fe–F bond of $Mb^{III}F$ compared to that of $Hb^{III}F$. This value compares to a 1-kcal experimentally observed increase for the $\Delta H$ of fluoride binding in $Hb^{III}F$ compared to that in $Mb^{III}F$ (Antonini & Brunori, 1971). However, the calculated and measured values are not necessarily directly related since differences in stored strain energy may exist for the aquo derivatives which are the reference states for the fluoride binding equilibrium studies.

It is not possible to calculate the difference in strain energy stored in the Fe–O bond of $Mb^{III}OH$ compared to that of $Hb^{III}OH$ since we do not know the force constant of this vibration in the corresponding non-protein-bound heme derivative. However, the smaller differences between the force constants of the Fe–O stretches in $Hb^{III}OH$ and $Mb^{III}OH$ compared to those of the Fe–F stretches in $Hb^{III}F$ and $Mb^{III}F$ indicate that the difference in stored strain energy between $Hb^{III}OH$ and $Mb^{III}OH$ must be smaller. A rough estimate made on the basis of the calculated bond elongations would result in a value of less than 0.5 kcal/mol but certainly positive since

$$\frac{\Delta S_{OH}}{\Delta S_F} = \frac{k_{OH}}{k_F}\left(\frac{\delta_{OH}^2 + 2\delta_{OH}X}{\delta_F^2 + 2\delta_F X}\right) \sim \frac{\delta_{OH}}{\delta_F}$$

where $\Delta S_{OH}$ ($\Delta S_F$) is the difference in strain energies stored in the Fe–O (Fe–F) bonds between methemoglobin(III) and metmyoglobin(III) hydroxide (fluoride) derivatives. $k_{OH}$ and $k_F$ are the force constants of the Fe–O and Fe–F bonds. These force constants are similar in value. $\delta_{OH}$ and $\delta_F$ are the differential elongations of the Fe–O and Fe–F bonds between the Hb(III) and Mb(III) derivatives, and $X$ which we consider identical between the fluoride and hydroxide derivatives is the

Table III: Spin-State Raman Frequencies and Heme Geometries in Low-Spin $Hb^{III}OH$ and $Mb^{III}OH$

| species | $\nu_a$ (cm$^{-1}$) | $\nu_b$ (cm$^{-1}$) | $R_{ct-N}$ (Å)$^a$ | $\phi$ (rad)$^a$ | $\psi$ (rad)$^a$ | $\Delta H^b$ (kcal) |
|---------|------|------|------|------|------|------|
| $Hb^{III}OH$ | 1636 | 1586 | 2.01 | 2.31 | 2.11 | -1.9 |
| $Mb^{III}OH$ | 1644 | 1592 | 1.99 | 2.26 | 2.13 | $-1.2 \pm 0.4$ |

$^a$ See the text and Figure 6 for definitions. $^b$ For high-spin ⇌ low-spin equilibrium (George et al., 1964).

elongation of the Fe–F and Fe–O bond from that in non-protein-bound heme derivatives. The calculated strain energies stored in the iron–axial ligand bonds are included in Table II.

As previously mentioned, the derived inverse-cube dependence of the force constant on the bond distance is relatively insensitive to the exact form used for the repulsive potential. If an exponential repulsive potential of the form $Be^{-r/\rho}$ is used, then

$$\frac{k_1}{k_2} = \left(\frac{r_2}{r_1}\right)^3 \frac{r_1 - 2\rho}{r_2 - 2\rho} \tag{7}$$

The cube dependence derives from the assumption that the major attractive influence is Coulombic. Because of this, it is unlikely that eq 5 would be as useful for covalently liganded complexes of heme proteins such as $HbO_2$ or the Fe–N (proximal histidine bond), $Fe-N_\epsilon$.

An empirical relationship first proposed by Badger (1934), modified by Herschbach & Laurie (1961), and utilized recently by Kincaid et al. (1979a) in their analysis of the Fe–N$_\epsilon$ bond

$$r = 0.85 + 1.5k^{-1/3}$$

results in bond lengths of 2.085 Å for $Hb^{III}OH$, 2.092 Å for $Mb^{III}OH$, 1.90 Å for $Fe^{III}PORF$, and 2.07 Å for $Hb^{III}F$. The bond elongations calculated from this empirical relationship are in the same direction but are about 50% smaller than those calculated from eq 5.

*Differences in Heme Geometry between Low-Spin $Mb^{III}OH$ and $Hb^{III}OH$.* The Raman data indicate a difference in heme macrocycle geometry between the low-spin species of met-hemoglobin and metmyoglobin hydroxide; the spin-state-sensitive Raman peaks of the low-spin $Hb^{III}OH$ species at 1636 and 1586 cm$^{-1}$ shift to 1644 and 1592 cm$^{-1}$ in $Mb^{III}OH$ (Figure 2).

Recently, Lanir et al. (1979) and Huong & Pommier (1977) have extended the work of Spaulding et al. (1975) and quantified the dependence of the Raman frequencies of the spin-state-sensitive modes on the average distance between the center of the heme and the pyrrole nitrogen atoms $R_{ct-N}$. Huong & Pommier (1977) have proposed the relationship $R_{ct-N}^a = 4.86 - 0.0018\nu_a$ for the anomalously polarized Raman peak occurring between 1550 and 1600 cm$^{-1}$ and $R_{ct-N}^b = 5.87 - 0.00236\nu_b$ for the depolarized Raman peak occurring between 1600 and 1650 cm$^{-1}$. Assuming a similar dependence, we can estimate that $R_{ct-N} = 1.99$ Å for the low-spin species of $Mb^{III}OH$ while $R_{ct-N} = 2.01$ Å for low-spin $Hb^{III}OH$ (Table III). Thus, there is an apparent contraction of 0.02 Å at the heme core from $Hb^{III}OH$ to $Mb^{III}OH$. In contrast, the frequencies of the Raman modes sensitive to the core size are the same within experimental error for the high-spin species of $Hb^{III}OH$ and $Mb^{III}OH$ and are very close to those frequencies observed for $Hb^{III}F$ and $Mb^{III}F$, indicating similar heme geometries.

We can estimate the difference in the internal energy of the heme between the low-spin species of $Mb^{III}OH$ and $Hb^{III}OH$ which is stored as bond and angle strains resulting from the
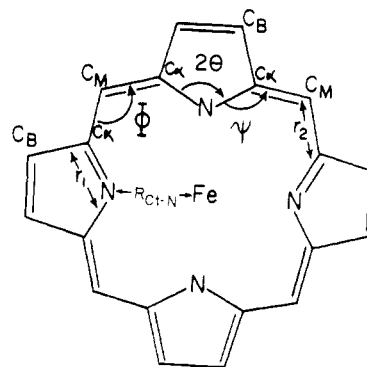


FIGURE 6: Schematic representation of heme structure labeling bond angles and distances.

heme core size changes. Since the force constants for changes in bond lengths are about a factor of 10 greater than for changes in bond angles [except for the metal–pyrrole nitrogen bond; Abe et al. (1978)], we can reasonably assume that except for the iron–pyrrole nitrogen bonds all bond lengths in the heme are conserved during the core expansion. If we further assume that the low-spin species have the iron atoms in plane and that the pyrroles all move rigidly outward from the center of the heme, we can calculate the angle subtended by the bonds linking the α-carbons of two different pyrrole rings to the methine carbon ($C_\alpha-C_M-C_\alpha$), $\phi$, and the angle subtended by the pyrrole nitrogen–α-carbon–methine carbon linkage ($C_N-C_\alpha-C_M$) (see Figure 6):

$$\phi = \pi - 2\cos^{-1}\left[\frac{2[R_{ct-N} - r_1(\cos\theta - \sin\theta)]^2}{2r_2}\right]^{1/2}$$

$$\psi = \frac{3\pi}{4} + \theta - \phi/2$$

where $\theta$ is half the angle between the bonds connecting the $C_\alpha$ carbons of one pyrrole and its pyrrole nitrogen, $r_1$ is the bond length between the α-carbon and the pyrrole nitrogen, and $r_2$ is the bond length between $C_\alpha$ and the methine carbon. Using the data of Abe et al. (1978) for the heme geometry ($r_1 = 1.38$ and $r_2 = 1.37$) but expanding the heme core to 1.99 and 2.01 Å for Mb(III) and Hb(III), respectively, we can calculate

$$\phi = 2.31 \quad \psi = 2.11 \text{ for } Hb^{III}OH$$

$$\phi = 2.26 \quad \psi = 2.13 \text{ for } Mb^{III}OH$$

The Raman and geometric data for the low-spin hydroxide complexes of Hb(III) and Mb(III) are summarized in Table III.

If energy storage in bond and angle deformations is assumed to occur as in a Hookes spring and if the heme geometry in $Hb^{III}OH$ is considered to be unstrained where all of the bond lengths and angles are those of unstretched springs, then

$$\Delta E = 2K(\Delta r_3)^2 + 2H_1r_2^2(\Delta\phi)^2 + 4H_2r_1r_2(\Delta\psi)^2$$

where $K$ is the stretching force constant for an iron–pyrrole nitrogen bond, $H_1$ is the bending force constant of the $C_\alpha-C_M-C_\alpha$ linkage, and $H_2$ is the bending force constant for the $N-C_\alpha-C_M$ link. Assuming the values of Abe et al. (1978), $k = 0.7$, $H_1 = 0.79$, and $H_2 = 0.32$ mdyn/Å where $\Delta r_3$, $\Delta\phi$, and $\Delta\psi$ are the extensions of the iron–pyrrole nitrogen bonds and the angle deformations in $Mb^{III}OH$ over those in $Hb^{III}OH$. This calculation results in $\Delta E = 8.9 \times 10^{-14}$ erg/mol or 1.3 kcal/mol of heme. We assume that the 2.01 Å $R_{ct-N}$ distance for low-spin $Hb^{III}OH$ indicates an unstrained heme since this distance is equivalent to the $R_{ct-N}$ distance in metalloporphyrins

which are thought to have minimal radial strain (Hoard, 1971).

The above calculation probably underestimates the strain energies stored in the bonds somewhat by assuming that $Hb^{III}OH$ is totally unstrained. If strain energy is present in $Hb^{III}OH$ stored as the bond elongations and angle deformations $\Delta r_3^0$, $\Delta\phi_0$, and $\Delta\psi_0$, the expression for $\Delta E$ must be modified:

$$\Delta E = 2K[(\Delta r_3)^2 + 2\Delta r_3\Delta r_3^0] + 2H_1 r_2^2[\Delta\phi^2 + 2(\Delta\phi)(\Delta\phi_0)] + 4H_2 r_1 r_2[\Delta\psi^2 + 2(\Delta\psi)(\Delta\psi_0)]$$

The presence of strain in $Hb^{III}OH$ would lead to an increase in $\Delta E$. For example, if the unstrained angle for the $C_\alpha$–$C_M$–$C_\alpha$ linkage were an unlikely 120°, $\Delta E$ would increase to 8.5 kcal.

An alternative approach for estimating the difference in heme strain energy resulting from differences in the heme core size results in a very similar 1.1-kcal energy difference between low-spin $Hb^{III}OH$ and low-spin $Mb^{III}OH$. If the spin-state-sensitive modes at ca. 1580 and 1640 cm$^{-1}$ result mainly from stretching of the methine bridge bonds (Spiro et al., 1979) and if changes in the force constant, $k$, scales with changes in the bond energy, $D$, then

$$\frac{\Delta k}{k} = \frac{\nu^2 - \nu'^2}{\nu^2} = \frac{\Delta D}{D}$$

where $\nu$ and $\nu'$ are the frequencies of the ca. 1580- or 1640-cm$^{-1}$ modes in $Mb^{III}OH$ and $Hb^{III}OH$, respectively. $D$ can be estimated as $\sim$115 kcal, the average of the 83- and 148-kcal bond energies of singly and doubly bonded carbon–carbon bonds, respectively (Cotton & Wilkinson, 1966). Then, $\Delta D$ $\sim$ 1.1 kcal.

*Implications for Heme–Globin Interactions.* The Raman data indicate that the iron lies further from the heme plane in the *high-spin* species of $Mb^{III}OH$ and $Mb(III)F$ than in the corresponding $Hb(III)$ derivatives and that the Fe–O bond elongation in $Mb^{III}OH$ over that in $Hb^{III}OH$ corresponds to an increase in strain energy $\Delta S_{Hb–Mb}^{HS} \simeq -0.5$ kcal/mol. The contraction in the heme core size between the *low-spin* hydroxide derivatives of $Hb(III)$ and $Mb(III)$ results in a strain energy difference of

$$\Delta S_{Hb–Mb}^{LS} \simeq -1.3 \text{ kcal/mol}$$

The enthalpy difference, $\Delta H$, between each of the spin species of $Mb(III)$ and $Hb(III)$ should be stored at the heme since the conversion rates between high- and low-spin species are too fast to allow for large protein conformational changes; the rates are similar to those observed for other inorganic iron complexes (Dose et al., 1977; Beattie et al., 1973; Beattie & West, 1974). $\Delta H$ should be directly related to differences in stored strain energy because any corresponding volume changes are small. The difference $\Delta(\Delta H)$ between the values of $\Delta H$ for the high-spin $\leftrightarrow$ low-spin equilibrium in $Hb^{III}OH$ and $Mb^{III}OH$ can be calculated by summing the differences in stored strain energy in the separate spin-state species:

$$\Delta(\Delta H) = \Delta H_{Hb} - \Delta H_{Mb} = (H_{Hb} - H_{Mb})^{LS} - (H_{Hb} - H_{Mb})^{HS} = \Delta S_{Hb–Mb}^{LS} - \Delta S_{Hb–Mb}^{HS} = -0.8 \text{ kcal/mol}$$

which is very close to the experimentally determined value of $-0.7$ kcal/mol (George et al., 1964).

$\Delta(\Delta H)$ shows the largest contribution from heme core contraction occurring in low-spin $Mb^{III}OH$. This contribution is partially canceled by the strain energy stored in the Fe–O bond of high-spin $Mb^{III}OH$. Thus, there appears to be additional stored strain energy in both the low- and high-spin species of $Mb^{III}OH$ over that in $Hb^{III}OH$. This additional energy must

result from interactions with the globin and could be due to an increased steric constraint present in $Mb^{III}OH$ which would result in the iron atom lying further to the proximal side of the heme plane and elongated Fe–$N_\epsilon$ and Fe–O bonds. In the low-spin species of $Mb^{III}OH$, nonbonded interactions of the proximal histidine with the pyrrole nitrogens would decrease relative to $Hb^{III}OH$, permitting the heme core to contract (Warshel, 1977b; Olafson & Goddard, 1977).

*Assignments of Low-Frequency Modes.* Attempts at observing the iron–proximal histidine stretch (Fe–$N_\epsilon$) to directly measure a tension at the heme iron have met with difficulty due to the weak enhancement shown by this mode. Recently, two groups have assigned this mode to two different Raman features. Desbois et al. (1978, 1979) assign the Fe–$N_\epsilon$ stretch in both oxidized and reduced myoglobin to a feature between 408 and 413 cm$^{-1}$ on the basis that this band is not observed in the IR spectra of metalloporphyrins or in the resonance Raman spectra of iron mesoporphyrin complexes. In contrast, Kincaid et al. (1979b) assign the Fe–$N_\epsilon$ stretch in deoxy-Hb-(II) and in deoxy-Mb(II) to a feature at 220 cm$^{-1}$ on the basis of the isotope shift observed upon deuterating the 2-methyl-imidazole complex of iron(III) protoporphyrin IX. They called their earlier 370-cm$^{-1}$ Fe–$N_\epsilon$ stretch assignment into question because of interference from vibrations of the methyl group in the 2-methylimidazole ligand (Kincaid et al., 1979b).

In a recent resonance Raman investigation of the imidazole complex of Mb(III), we observed a selective enhancement of peaks at 385 and 519 cm$^{-1}$ in conjunction with peaks indicative of a high-spin iron (Asher and Schuster, unpublished experiments). We do not observe significant enhancement of a Raman peak around 220 cm$^{-1}$. In view of the analogous enhancement of axial ligand modes in the OH$^-$, F$^-$, and N$_3^-$ heme derivatives, it is tempting to assign either the 385- or possibly the 519-cm$^{-1}$ peak to the Fe–imidazole stretch, especially since the frequency of an analogous peak (ca. 380 cm$^{-1}$) occurring in the resonance Raman spectra of $Mb^{III}OH$ and $Hb^{III}OH$ shows a 6-cm$^{-1}$ *increase* from $Mb^{III}OH$ (382 cm$^{-1}$) to $Hb^{III}OH$ (388 cm$^{-1}$) (Figure 4). However, we also see a 4-cm$^{-1}$ *increase* for the peak occurring at 414 cm$^{-1}$ in $Mb^{III}OH$ to 418 cm$^{-1}$ in $Hb^{III}OH$. The shifts in frequency of these Raman peaks from $Hb^{III}OH$ and $Mb^{III}OH$ are in the correct direction if either of these features correspond to the Fe–$N_\epsilon$ stretch; the increasing displacement of the iron atom from the heme plane, which results in a decreased force constant and presumably an increased bond length for the Fe–O bond in $Mb^{III}OH$, would be expected to correlate with an elongation of the Fe–$N_\epsilon$ bond. In contrast, Kincaid et al. (1979a) saw little or no shift in the 220-cm$^{-1}$ mode from deoxy-Mb(II) to deoxy-Hb(II).

The frequencies of both the 410- and 380-cm$^{-1}$ peaks are essentially independent of the sixth axial ligand or of the spin state of the heme (Desbois et al., 1978, 1979). However, these peaks do show small shifts (<5 cm) upon conversion between the ferric and ferrous forms. The essential invariance of either of these features to the sixth axial ligand or to the spin-state changes within either hemoglobin or myoglobin is disappointing. If either the 380- or 410-cm$^{-1}$ assignment to the Fe–$N_\epsilon$ stretch is correct, it appears that the proximal histidine can easily follow the heme iron into or out of the heme plane and that there is no "tension" at the iron due to the proximal histidine–iron linkage.

It is, however, possible that neither of these modes corresponds to the Fe–$N_\epsilon$ stretch and that they instead correspond to modes containing large contributions from the iron–pyrrole nitrogen linkages. These modes would also be expected to be

sensitive to movements of the iron away from the heme plane, decreasing in frequency as the iron–pyrrole nitrogen bonds lengthen. However, they may be less sensitive than the Fe–N$_\epsilon$ linkage. Alternatively, the observed modes may represent admixtures of Fe–N$_\epsilon$ and iron–pyrrole nitrogen stretches. Whatever the assignment for these modes, it is satisfying that they show a decrease in frequency from deoxy-Mb(II) to deoxy-Hb(II) and an increase from Mb$^{III}$OH to Hb$^{III}$OH; from X-ray data it is known that the iron lies farther from the heme plane in deoxy-Hb(II) than in deoxy-Mb(II) and farther in aquo-Mb(III) than in aquo-Hb(III) (Takano, 1977a,b; Ladner et al., 1977).

## Conclusions

The simultaneous selective enhancement in Mb$^{III}$X$^-$ and Hb$^{III}$X$^-$ (X = OH$^-$, F$^-$, N$_3^-$) of Fe–X stretches and "high-spin" porphyrin macrocycle modes upon excitation in the ca. 6000-Å charge-transfer bands indicates that these electronic transitions are derived from the high-spin species within the spin-state equilibria of these derivatives. No iron–axial ligand modes are observed for the low-spin species. The Raman cross section for the iron–axial ligand stretches is correlated with the magnitude of the out-of-plane component of the charge-transfer transition which is related to the out-of-plane iron distance.

The decrease in the force constant of the Fe–X (X = OH$^-$, F$^-$) stretches from Hb$^{III}$X to Mb$^{III}$X indicates 0.01- and 0.05-Å elongations of the Fe–X bond lengths in Mb$^{III}$OH and Mb$^{III}$F from those in Hb$^{III}$OH and Hb$^{III}$F, respectively. These elongations are presumed to result from an increased displacement of the iron from the heme plane in Mb$^{III}$OH and Mb$^{III}$F from that in Hb$^{III}$OH and Hb$^{III}$F. Calculations of the strain energy stored in the Fe–F bonds of Mb$^{III}$F and Hb$^{III}$F indicate an increase of 2 kcal/mol of heme in Mb$^{III}$F, which may partially account for the experimentally observed 1.0 kcal/mol of heme decrease in the F$^-$ binding enthalpy from Hb$^{III}$F to Mb$^{III}$F.

The Raman data indicate that the low-spin species of Mb$^{III}$OH has a smaller heme core size than the low-spin species of Hb$^{III}$OH. Calculations of the differences in strain energy stored in the heme macrocycle and in the Fe–O bonds between Mb$^{III}$OH and Hb$^{III}$OH result in a total strain energy difference of 0.8 kcal/mol of heme which is close to the 0.7 kcal/mol of heme difference measured by others for the $\Delta H$ difference between Mb$^{III}$OH and Hb$^{III}$OH in the two high-spin ↔ low-spin equilibria.

This work illustrates the sensitivity of iron–axial ligand modes to changes in protein structure and supports the conclusion of Asher et al. (1977) that in high-spin Hb$^{III}$F essentially no movement of the iron occurs with respect to the heme plane (<0.01 Å) upon conversion of Hb$^{III}$F from the R to the T form by InsP$_6$.

## Acknowledgments

## References

Abe, M., Kitagawa, T., & Kyogoku, Y. (1978) *J. Chem. Phys. 69*, 4526.

Alben, J. O., & Fager, L. Y. (1972) *Biochemistry 11*, 842.

Albrecht, A. C. (1971) *J. Chem. Phys. 34*, 1476.

Antonini, E., & Brunori, M. (1971) *Hemoglobin and Myoglobin in Their Reactions with Ligands: Frontiers of Bi-*

*ology* (Neuberger, A., & Tatum, E. L., Eds.) Vol. 21, North-Holland Publishing Co., Amsterdam.

Asher, S. A. (1976) Ph.D. Thesis, University of California, Berkeley, Report LBL-5375.

Asher, S., & Sauer, K. (1976) *J. Chem. Phys. 64*, 4115.

Asher, S. A., & Schuster, T. M. (1979) *Biophys. J. 25*, 127a (abstract only).

Asher, S. A., Vickery, L. E., Schuster, T. M., & Sauer, K. (1977) *Biochemistry 16*, 5849.

Badger, R. M. (1934) *J. Chem. Phys. 2*, 128.

Beattie, J. K., & West, R. J. (1974) *J. Am. Chem. Soc. 96*, 1933.

Beattie, J. K., Sutin, N., Turner, D. H., & Flynn, G. W. (1973) *J. Am. Chem. Soc. 95*, 2052.

Beetlestone, J., & George, P. (1964) *Biochemistry 3*, 707.

Brunner, H. (1974) *Naturwissenschaften 61*, 129.

Chottard, G., & Mansuy, D. (1977) *Biochem. Biophys. Res. Commun. 77*, 1333.

Cotton, F. A., & Wilkinson, G. (1966) *Advanced Inorganic Chemistry*, Wiley, New York.

Deatherage, J. F., Loe, R. S., & Moffat, K. (1976) *J. Mol. Biol. 104*, 723.

Desbois, A., Lutz, M., & Banerjee, R. (1978) *C. R. Hebd. Seances Acad. Sci., Ser. D 287*, 349.

Desbois, A., Lutz, M., & Banerjee, R. (1979) *Biochemistry 18*, 1510.

Dose, E. V., Tweedle, M. F., Wilson, L. J., & Sutin, N. (1977) *J. Am. Chem. Soc. 99*, 3886.

Eaton, W. A., & Hochstrasser, R. M. (1968) *J. Chem. Phys. 49*, 985.

Fleisher, E. B., Miller, C. K., & Webb, L. E. (1964) *J. Am. Chem. Soc. 86*, 2342.

George, P., Beetlestone, J., & Griffith, J. S. (1961) in *Haematin Enzymes* (Falk, J. E., Lemberg, R., & Morton, R. K., Eds.) p 105, Pergamon Press, New York.

George, P., Beetlestone, J., & Griffith, J. S. (1964) *Rev. Mod. Phys. 36*, 441.

Hapner, K. D., Bradshaw, R. A., Hartzell, C. R., & Gurd, F. R. N. (1968) *J. Biol. Chem. 243*, 683.

Herschbach, D. R., & Laurie, V. W. (1961) *J. Chem. Phys. 35*, 458.

Hoard, J. L. (1971) *Science 174*, 1295.

Hoard, J. L., Hamor, M. J., Hamor, T. A., & Caughey, W. S. (1965) *J. Am. Chem. Soc. 87*, 2312.

Huong, P. V., & Pommier, J.-C. (1977) *C. R. Hebd. Seances Acad. Sci., Ser. C 285*, 519.

Iizuka, T., & Kotani, M. (1969a) *Biochim. Biophys. Acta 181*, 275.

Iizuka, T., & Kotani, M. (1969b) *Biochim. Biophys. Acta 194*, 351.

Iizuka, T., & Yonetani, T. (1970) *Adv. Biophys. 1*, 157.

Kincaid, J., & Nakamoto, K. (1976) *Spectrosc. Lett. 9*, 19.

Kincaid, J., Stein, P., & Spiro, T. G. (1979a) *Proc. Natl. Acad. Sci. U.S.A. 76*, 549.

Kincaid, J., Stong, J. D., & Spiro, T. G. (1979b) *Proc. Natl. Acad. Sci. U.S.A.* (in press).

Kitagawa, T., Kyogoku, Y., Iizuka, T., & Saito, M. I. (1976) *J. Am. Chem. Soc. 98*, 5169.

Kittel, C. (1971) *Introduction to Solid State Physics*, Wiley, New York.

Ladner, R. C., Heidner, E. J., & Perutz, M. F. (1977) *J. Mol. Biol. 114*, 385.

Lanir, A., Yu, N.-T., & Felton, R. H. (1979) *Biochemistry 18*, 1656.

McCoy, S., & Caughey, W. S. (1970) *Biochemistry 9*, 2387.

Messana, C., Cerdonio, M., Shenkin, P., Noble, R. W., Fermi, G., Perutz, R. N., & Perutz, M. F. (1978) *Biochemistry 17*, 3652.

Morimoto, H., & Kotani, M. (1966) *Biochim. Biophys. Acta 126*, 176.

Ogoshi, H., Watenabe, E., Yoshida, Z., Kincaid, J., & Nakamoto, K. (1973) *J. Am. Chem. Soc. 95*, 2845.

Olafson, B. D., & Goddard, W. A. (1977) *Proc. Natl. Acad. Sci. U.S.A. 74*, 1315.

Ozaki, Y., Kitagawa, T., & Kyogoku, Y. (1976) *FEBS Lett. 62*, 369.

Perutz, M. F., Heidner, E. J., Ladner, J. E., Beetlestone, J. G., Ho, C., & Slade, E. F. (1974) *Biochemistry 13*, 2187.

Perutz, M. F., Sanders, J. K. M., Chenery, D. H., Noble, R. W., Pennelly, R. R., Fung, L. W.-M., Ho, C., Giannini, I., Porschke, D., & Winkler, H. (1978) *Biochemistry 17*, 3640.

Smith, D. W., & Williams, R. J. P. (1968) *Biochem. J. 110*, 297.

Smith, D. W., & Williams, R. J. P. (1970) *Struct. Bonding (Berlin) 7*, 1.

Spaulding, L. D., Chang, C. C., Yu, N.-T., & Felton, R. H. (1975) *J. Am. Chem. Soc. 97*, 2517.

Spiro, T. G. (1975) *Biochim. Biophys. Acta 416*, 169.

Spiro, T. G., & Burke, J. M. (1976) *J. Am. Chem. Soc. 98*, 5482.

Spiro, T. G., Stong, J. D., & Stein, P. (1979) *J. Am. Chem. Soc. 101*, 2648.

Strekas, T. C., & Spiro, T. G. (1974) *Biochim. Biophys. Acta 351*, 237.

Strekas, T. C., Adams, D. H., Packer, A. J., & Spiro, T. G. (1974) *Appl. Spectrosc. 28*, 234.

Takano, T. (1977a) *J. Mol. Biol. 110*, 537.

Takano, T. (1977b) *J. Mol. Biol. 110*, 569.

Warshel, A. (1977a) *Annu. Rev. Biophys. Bioeng. 6*, 273.

Warshel, A. (1977b) *Proc. Natl. Acad. Sci. U.S.A. 74*, 1789.

Williams, R. C., Jr., & Tsay, K.-Y. (1973) *Anal. Biochem. 54*, 137.

Yonetani, T., Iizuka, T., & Waterman, M. R. (1971) *J. Biol. Chem. 246*, 7683.

Yu, N.-T. (1977) *CRC Crit. Rev. Biochem. 4*, 229.

# Nitric Oxide and Carbon Monoxide Equilibria of Horse Myoglobin and (N-Methylimidazole)protoheme. Evidence for Steric Interaction with the Distal Residues[†]

Robert W. Romberg and Richard J. Kassner*

ABSTRACT: The Soret absorption maxima and extinction coefficients of the CO and NO complexes of horse myoglobin and (NMeIm)protoheme (NMeIm = 1-methylimidazole) have been determined. The partition coefficient $N$, equal to the ratio $P_{1/2}(CO)/P_{1/2}(NO)$, has been determined spectrophotometrically for horse myoglobin and (NMeIm)protoheme. $P_{1/2}(NO)$ values calculated from the partition coefficients are 5.7 × 10$^{-7}$ mmHg for (NMeIm)protoheme and 1.1 × 10$^{-6}$ mmHg for horse myoglobin. The ratio of $P_{1/2}(NO)$ values for protein and model is 1.9 which is similar to a value of 1.6 reported for the ratio of $P_{1/2}(O_2)$ values. These values may be compared to a ratio of 15 for CO binding to protein and model complexes. This different ratio for CO provides further evidence for steric interaction of the bound CO with the protein based on a consideration of the preferred nonlinear geometry of Fe–NO and Fe–O$_2$ and the linear geometry of Fe–CO.

**D**ata on infrared stretching frequencies have been extremely important in revealing the nature of protein ligand bonds. Over the last several years the literature has provided CO infrared stretching frequencies of various hemoproteins (Caughey, 1970; Caughey et al., 1969; Alben & Caughey, 1968). Many normal hemoglobins exhibit similar CO frequencies, but abnormal hemoglobins with the distal histidine replaced by amino acid residues bearing hydrophilic side chains have considerably higher CO frequencies (Caughey et al., 1969). The stretching frequencies of these mutant hemoglobins approach the $\nu_{CO}$ of model heme complexes (Collman et al., 1976).

Differences in the $\nu_{CO}$ have been interpreted in terms of the structure and ligand binding properties of hemoprotein and model complexes. The Fe–CO bond has been found to be linear in the nonhindered model systems Fe(TpivPP)(NMeIm)CO[1] (Hoard, 1975) and Fe(TPP)(py)CO (Peng & Ibers, 1976). X-ray data (Huber et al., 1970; Padlan & Love, 1974) indicate that in proteins the CO to Fe bond is bent or tilted. A neutron diffraction study has indicated a Fe–C–O bond angle of 135° in horse myoglobin (Norvell et al., 1975). These studies indicate that amino acid residues in the heme pocket are close enough to cause CO to bend or tilt from its preferred linear structure. Specifically, valine (residue E11) and the distal histidine (residue E7) are capable of interacting with CO when it is bound to horse myoglobin (Norvell et al., 1975). Caughey has attributed the lower $\nu_{CO}$ in normal hemoglobins and myoglobins to a donation of electron density from the nitrogen of the distal histidine to the partially electropositive carbon atom of the bent or tilted CO molecule (Caughey, 1970). Collman has suggested that the lower stretching frequencies result from steric hindrance which distorts the CO from its preferred linear structure (Collman et al., 1976).

[1] Abbreviations used: NMeIm, 1-methylimidazole; PP, protoporphyrinate; TpivPP, *meso*-tetrakis($\alpha,\alpha,\alpha,\alpha$-*o*-pivalamidophenyl)porphyrinate; NTrIm, 1-tritylimidazole; py, pyridine; $P_{1/2}$, partial pressure of gas at half-saturation; Mb, myoglobin; Im, imidazole; TPP, *meso*-tetraphenylporphyrinate; CTAB, cetyltrimethylammonium bromide.